The British Journal of Radiology, 83 (2010), 290–295

Investigation of the effect of anode/filter materials on the dose and image quality of a digital mammography system based on an amorphous selenium flat panel detector

P BALDELLI, PhD, N PHELAN, MSc and G EGAN, MSc

Breastcheck, The National Cancer Screening Service, 36 Eccles Street, Dublin, Ireland

ABSTRACT. A comparison, in terms of image quality and glandular breast dose, was carried out between two similar digital mammography systems using amorphous selenium flat panel detectors. The two digital mammography systems currently available from Lorad-Hologic were compared. The original system utilises Mo/Mo and Mo/Rh as target/filter combinations, while the new system uses W/Rh and W/Ag. Images of multiple mammography phantoms with simulated compressed breast thicknesses of 4 cm, 5 cm and 6 cm and various glandular tissue equivalency were acquired under different spectral conditions. The contrast of five details, corresponding to five glandular compositions, was calculated and the ratio of the square of the contrast-to-noise ratio to the average glandular dose was used as a figure-of-merit (FOM) to compare results. For each phantom thickness and target/filter combination, there is an optimum voltage that maximises the FOM. Results show that the W/Rh combination is the best choice for all the detection tasks studied, but for thicknesses greater than 6 cm the W/Ag combination would probably be the best choice. In addition, the new system with W filter presents a better optimisation of the automatic exposure control in comparison with the original system with Mo filter.

Received 28 February 2008
Revised 12 July 2009
Accepted 10 August 2009

DOI: 10.1259/bjr/60404532

Over the past decade, several digital mammography systems based on different detector technologies have become available and the process of optimisation of digital systems has been developing in parallel with the adoption of those systems. On the one hand, this process involves the optimisation of digital detectors, but, on the other hand, it involves the optimisation of the X-ray sources and exposure factors with regards to the minimum radiation dose required to maintain the highest possible image quality. In conventional mammography this optimisation has mostly been achieved using the anode/filter combination Mo/Mo, but it may be questioned whether it is also optimal for digital mammography.

In the past few years, several studies and simulation works have been carried out in order to investigate the factors that affect choice of X-ray spectra for mammography.

Dance et al [1] in their Monte Carlo study concluded that in digital mammography with a gadolinium oxysulphide detector, the standard Mo/Mo combination is superior only for 2 cm compressed breasts. For all other compressed breast thicknesses and glandularities, each of the alternative anode/filter combinations (Mo/Rh, W/Rh, Rh/Rh and Rh/Al) can offer a lower dose for the same contrast-to-noise ratio (CNR). In particular, for compressed breast thicknesses of 4 cm to 6 cm, W/Rh is recommended.

Address correspondence to: P Baldelli, Breastcheck, The National Cancer Screening Service, 36 Eccles Street, Dublin, Ireland. E-mail: paola.baldelli@gmail.com

In a previous work, Andre and Spivey [2] developed a parametric model for digital mammography to evaluate optimisation of X-ray spectra for a particular sensor. The model computes spectra and average glandular doses (AGD) for combinations of W target, beam filters (Al, Sn, Rh, Mo and Ag), kVp, breast type and thickness. On the basis of their results, the authors suggest the use of Mo filter for 30 mm breast, Ag filter for 45 mm, Sn filter for 60 mm and Al filter for 75 mm breast thicknesses.

Fahrig and Yaffe [3, 4], in their simulation study, demonstrated that using a digital detector based on Gd_2O_2S scintillator, a W target is preferable to a Mo target for the detection of infiltrating ductal carcinoma and calcifications.

In the work of Flynn and colleagues [5], the radiographic process for a digital amorphous selenium (aSe) mammography system was modelled. The optimal CNR relative to dose was determined for several target/filter combinations, for a wide range of kVp values, and for varying breast thickness. The target/filter combinations included Mo/Mo, Mo/Rh, Rh/Rh, W/Al, W/Mo, W/Ag and W/Sn. Results show that when breast thickness increased, the use of a W target with a Sn filter resulted in a 34% improvement in CNR for the same dose to the breast compared with the use of a Mo target with a Mo filter.

In their recent work, Bernhardt et al [6] related the image quality and patient risk through simulations and phantom studies regarding the detection of microcalcifications and tumours for different breast thickness and breast compositions, anode/filter combinations, different filter thicknesses and different tube voltages. They found that, for an aSe detector, the W/Rh target/filter combination is

the best choice for all breast thicknesses and composition and for the detection of both microcalcifications and tumours.

Similar results were found by Toroi et al [7], who measured the CNR between aluminium sheets and homogeneous background for various radiation qualities and breast thicknesses to determine the optimal radiation quality when using an aSe detector based system. By using a W anode in combination with an Rh filter, they achieved the same CNR with a significantly lower dose than when using Mo anode with an Mo or Rh filter. This result is valid for all breast thicknesses, but is most significant for the thickest breasts.

In a recent paper Williams et al [8] compared, for each of the major commercially available full-field digital mammography (FFDM) systems, the impact of the selection of exposure factors on image quality and dose for a range of breast thickness and tissue types. They used the figure-of-merit (FOM) (signal-to noise ratio^2/mean glandular dose (MGD)) to compare the technique factors of all available target/filter combinations. A key finding of their study was the better performance of W/Rh combinations, as compared with Mo/Mo and Mo/Rh combinations, using the same aSe detector.

Given these and other similar published results, manufacturers have introduced mammography units with different anode/filter combinations, such as Mo/Rh, Rh/Rh, W/Rh and W/Ag, and the process of optimisation is on-going.

In particular, Lorad-Hologic (Hologic Inc., Danbury, CT) has recently introduced to the market a new Selenia digital mammography system. The new system is very similar to the previous system and differs primarily in respect of the target/filter combinations available – it consists of an X-ray tube with W anode material combined with Rh and Ag filter materials.

The aims of this study were twofold. One goal was to establish optimum spectra for breasts of different thicknesses and compositions imaged with both the original and the new Lorad system. In addition, we aimed to compare the two generations of Lorad system in terms of X-ray spectra to the optimum.

Methods and materials

The two digital mammography systems currently available from Lorad-Hologic were used throughout this study. The original system consists of an X-ray tube with Mo anode material with Mo and Rh filter materials (30 μm and 25 μm thick, respectively) and an aSe direct conversion flat panel detector. The pixel matrix is 3328 $\times$ 4096 pixels with a pixel pitch of 70 μm for a 24 $\times$ 29 cm active image area. In the new system, the Mo anode has been replaced with a W anode. A 50 μm thick Rh filter or a 50 μm thick Ag filter can be used. The automatic exposure control (AEC) is programmed to maintain constant pixel value (PV) as thickness is varied and has three modes of operation: standard dose, low dose and limited dose. The system evaluated in this work was set up in standard dose.

CIRS phantoms (CIRS, Inc., Norfolk, VA) of breast equivalent material at different thickness and composition were used to compare the performance of the systems in terms of dose and contrast. Phantoms are breast-shaped and made of epoxy tesin, with standard thickness taken as 40–60 mm, equivalent to 50%, 30% and 20% glandular breast tissue, respectively, in terms of its X-ray attenuation properties. Among various details included in the phantom, we used the step wedge for contrast measurements. It consists of five details, 1 cm thick, corresponding to glandular compositions of 0%, 30%, 50%, 70% and 100%. Close to the step wedge, a reference zone in a uniform region of the phantom for the measurement of the pixel value is highlighted. A schematic diagram of the phantom is shown in Figure 1. Special attention was given to placement of the phantom in the same position on the detector and the uniformity of the detector was measured according to the European guidelines [9]. For both mammography systems the maximum deviation in pixel value over the entire detector area was $<5\%$.

Images of the phantoms were acquired in manual mode for both mammography systems, using peak tube voltages ranging from 24 to 34 at intervals of 2 kV. Tube current–time product (mAs) values were chosen in order to obtain a constant pixel value level in the reference zone similar to that obtained by the system working in automatic exposure control. For each detail, the CNR was calculated according to the definition in the European guidelines for quality assurance in mammography screening [9]:

$$\mathrm{CNR} = \frac{\mathrm{PV_B} - \mathrm{PV_d}}{\sqrt{\frac{\sigma_B^2 + \sigma_d^2}{2}}} \quad (1)$$

where $\mathrm{PV_B}$ is the pixel value measured in the reference zone, $\mathrm{PV_d}$ is the pixel value measured in an area of 6 $\times$ 6 mm in the detail area, and σ_B and σ_d are the standard deviations.

For each setting, half value layer (HVL) and entrance surface air kerma (ESAK) were measured and the corresponding MGD was calculated according to Dance et al [10] using the formula:

$$\mathrm{MGD} = K \cdot g \cdot c \cdot s \quad (2)$$

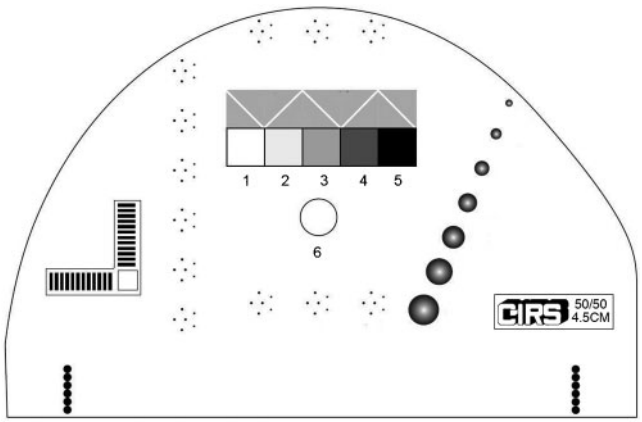

Figure 1. Schematic diagram of a CIRS phantom. The step wedge for the CNR measure is represented by details 14–18: detail 14, 100% glandular; detail 15, 70% glandular; detail 16, 50% glandular; detail 17, 30% glandular; detail 18, 100% adipose. The region of interest (ROI) 31 is the reference ROI.

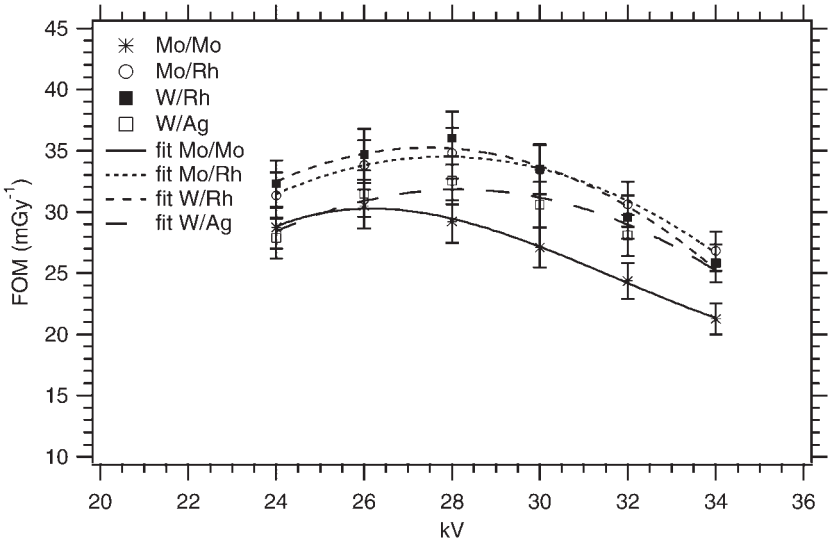

Figure 2. Figure-of-merit (FOM) as a function of tube voltage. Results refer to a detail 100% glandular embedded in a phantom 4 cm thick, 50% glandular.

where K is the ESAK at the upper surface of the breast and g, c and s depend on both X-ray beam and breast characteristics. For the W/Ag configuration, we used an s-factor value of 1.063 according to the recent results of Dance and Young (personal communication). We used c-factors corresponding to a glandularity of equivalent breast of 50%, 30% and 20%, according to the CIRS phantom specifications. The absolute uncertainty of the AGD measurement was estimated to be 16%, based on the uncertainty in the measurement of air kerma using the ionisation chamber and the error estimations reported by Dance et al [10]. The optimisation of the spectra and the comparison of the two generations of systems were based on the FOM commonly used for mammographic beam optimisation studies [11, 12], and defined as:

$$\mathrm{FOM} = \frac{\mathrm{CNR}^2}{\mathrm{MGD}} \qquad (3)$$

Assuming that the two mammographic systems are quantum-limited, the FOM is independent of the dose level. Higher values of the FOM indicate the ability of the system to deliver better performance in terms of image quality at a lower dose and it is useful to establish the best acquisition setting for a given mammographic system.

The FOM was calculated for all acquisition conditions and plotted as a function of kV for the three phantom thicknesses.

An optimal peak tube voltage was determined by taking the maximum value of the FOM for each target/filter combination. These values were compared with those chosen by the systems when operating in automatic mode in order to test the optimisation of the AEC mode of the systems.

Results

Full results for the 100% glandular detail, which simulate a typical tumour density, are presented. For each breast model (thickness and glandularity), the FOM was plotted against the tube potential for each target/filter combination. Figures 2, 3 and 4, respectively, show results for compressed breasts of 4 cm thickness and 50% glandularity, 5 cm thickness and 30% glandularity, and 6 cm thickness and 20% glandularity. In the graphs for

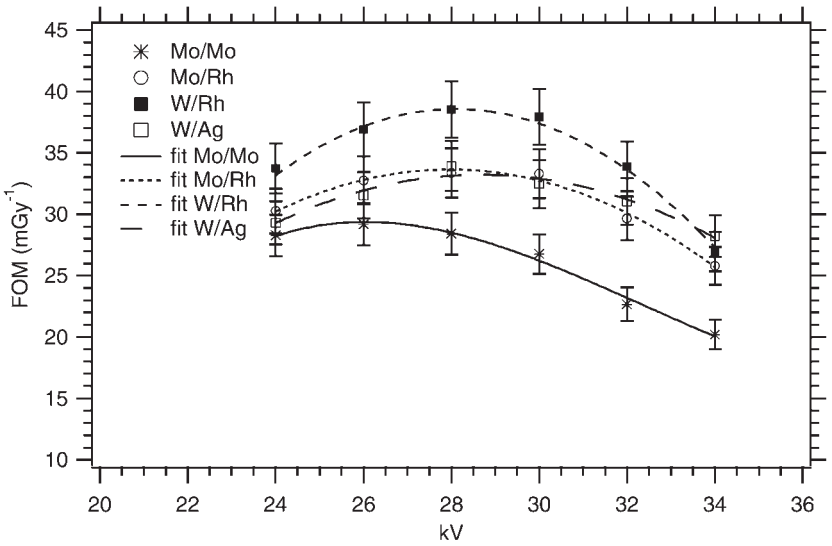

Figure 3. Figure-of-merit (FOM) as a function of tube voltage. Results refer to a detail 100% glandular embedded in a phantom 5 cm thick, 30% glandular.

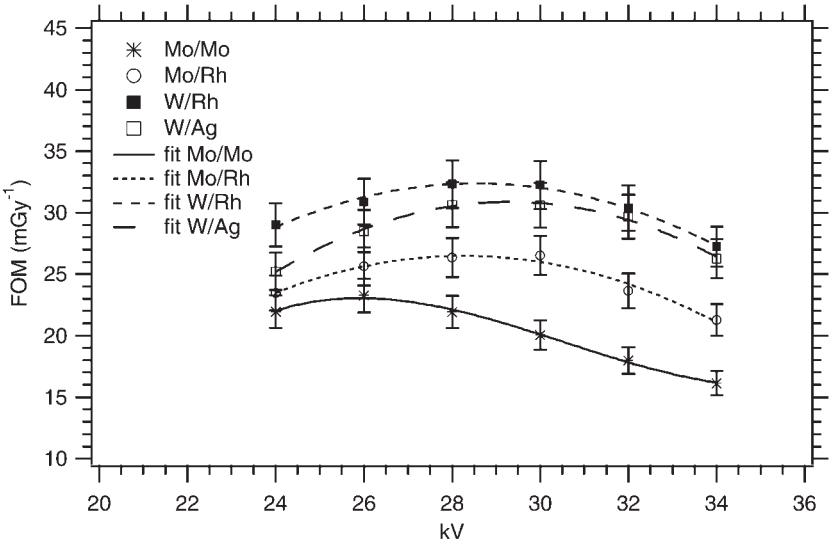

Figure 4. Figure-of-merit (FOM) as a function of tube voltage. Results refer to a detail 100% glandular embedded in a phantom 6 cm thick, 20% glandular.

each target/filter combination, there is an optimum voltage at which the FOM reaches its maximum. Graphs were fitted with second-order polynomial curves and the R^2 values range between 0.980 and 0.999. The highest maximum for all anode/filter combinations is the optimal combination for the particular breast model.

Table 1 demonstrates the tube potential value that maximises the FOM for each target/filter combination and each breast model. MGD values required to achieve the target PV in the reference zone are also reported. For each breast model, the value in bold is the optimal combination for the particular model. These values were compared with the values chosen under fully AEC mode of the systems. Results are reported in Table 2.

Discussion

Results reported in Figures 2, 3 and 4 show that for each breast model and target/filter combination the curves have a similar shape. The curves for W/Rh are always the highest, whereas those for Mo/Mo are always the lowest. In particular, for the Mo/Mo combination the optimum tube potential is 2–4 kV lower with respect to the other combinations, for each breast thickness. This means that the W/Rh combination is always the best choice, whereas the Mo/Mo combination is always the least suitable choice for the optimisation of the acquisition. The Mo/Rh curve is similar to the W/Rh curve at 4 cm and with the W/Ag curve at 5 cm, but it is lower at 6 cm. The W/Ag curve comes near to the W/Rh curve by increasing the thickness of the phantom.

By using the data reported in Table 1, it is possible to compare the performances of each target/filter combination working at the optimum tube potential value. The dose reduction discussed is that obtained for images with the same pixel value in the reference zone. In particular, using the W/Rh combination with tube potential values of 28 kV at 4 cm, 29 kV at 5 cm and 30 kV at 6 cm, there is an increase in the FOM ranging from 18% to 39%, with a dose reduction ranging from 40% to 53%, when compared with the Mo/Mo combination at 26 kV. The comparison with the Mo/Rh combination for every thickness results in an increase in the FOM ranging from 4% to 22% with a reduction of the dose ranging from 10% to 26%.

As far as the comparison of W/Rh and W/Ag is concerned, it is possible to achieve an increase in the FOM of 10% at 4 cm, 14% at 5 cm and 5% at 6 cm with a W/Rh combination, but in this case there is an increase in the dose of 40% at 4 cm, 23% at 5 cm and 20% at 6 cm. In fact, the W/Ag combination produces more penetrating X-ray beams which present a higher value of HVL and then a lower value of MGD.

The preferred combination for the particular breast model can be used to evaluate the optimisation of the AEC of the two systems, as demonstrated in Table 2. The Se-Mo tube system favours the Mo/Mo combination at 27–31 kV, but the more optimal choice would be Mo/Rh at 28–29 kV depending on the thickness. The choice of the AEC provides an FOM 27% less than those estimated with the optimal parameters. By contrast, the Selenia-W tube system successfully identifies exposure parameters resulting in FOM close to maximum. In particular, the AEC choice ranges from 27 kV to 29 kV, which is close to the estimated optimisation of 28–30 kV. The AEC of the new system provides an FOM 15% less at 4 cm and 8% less at 6 cm than the estimated optimal parameters.

We assumed in this work that the FOM is independent of the dose level. If electronic or structural noise contributes to the total noise in addition to quantum noise, some results could be different. In particular, the FOM calculated for higher dose values could be lower. However, as the detector incorporated by the two systems is the same, the comparison between the results is still valid.

Our results may be compared and are in good agreement with those of other work. Bernhardt et al [6] based their work on parameter optimisation for the detection of microcalcifications and tumours at different breast thicknesses and compositions using three different anode/filters combinations. They reported that for a digital mammography system based on an aSe detector, the W/Rh combination is the best choice for all detection tasks studied. Specifically, for tumour detection they found that for a 4 cm breast thickness and 50% glandular composition, the optimal tube voltages for the Mo/Mo, Mo/Rh and W/Rh combinations are 26.5 kV, 28.5 kV

Table 1. Optimised parameters for the Mo and W target based systems

CIRS phantom	Original system						New system					
	Mo/Mo	FOM (mGy^{-1})	MGD (mGy)	Mo/Rh	FOM (mGy^{-1})	MGD (mGy)	W/Rh	FOM (mGy^{-1})	AGD (mGy)	W/Ag	FOM (mGy^{-1})	MGD (mGy)
4 cm	26 kV	30.5±1.9	1.22±0.18	28 kV	34.8±2.2	0.83±0.12	28 kV	36±2.3	0.74±0.11	28 kV	32.5±2.1	0.53±0.08
5 cm	26 kV	29.2±1.9	1.72±0.26	28 kV	33.4±2.1	1.14±0.17	29 kV	38.3±2.4	0.88±0.13	29 kV	33.2±2.4	0.71±0.11
6 cm	26 kV	23.2±1.4	2.46±0.37	29 kV	26.4±1.6	1.55±0.23	30 kV	32.2±2.1	1.15±0.17	29 kV	30.6±1.9	0.96±0.14

MGD, mean glandular dose; FOM, figure-of-merit.

Table 2. Parameters chosen under fully automatic exposure control mode by the Mo and W target based systems

CIRS phantom	Original system			New system		
	AEC mode	FOM (mGy^{-1})	MGD (mGy)	AEC mode	FOM (mGy^{-1})	MGD (mGy)
4 cm	Mo/Mo 27 kV	25.74	1.46±0.22	W/Rh 27 kV	30.9±1.8	0.98±0.15
5 cm	Mo/Mo 29 kV	24.38	1.49±0.22	W/Rh 28 kV	33.4±1.9	1.19±0.19
6 cm	Mo/Mo 31 kV	19.04	1.69±0.24	W/Rh 29 kV	29.8±1.8	1.48±0.23

MGD, mean glandular dose; FOM, figure-of-merit.

and 28 kV, respectively; we found these to be 26 kV for Mo/Mo, 28 kV for Mo/Rh and 28 kV for W/Rh.

The optimum tube voltages estimated in our work are also in good agreement with those estimated by Toroi et al [7], who indicate the lowest and highest acceptable tube voltages for every thickness. They also conclude that the WRH combination provided, at a parity of image quality, a lower dose.

In a study by Williams et al [8], a comparison of the two systems based on an aSe detector led to the conclusion that for all breast types the FOM values obtained by the system using the W/Rh combination are superior to those using either Mo/Mo or Mo/Rh. In addition, their results show that the Selenia-Mo system produces maximum FOM values for nearly all breast types at an exposure parameter setting of Mo/Rh 27 kV, with only a slightly higher voltage (Mo/Rh 28 kV) for the densest 7 cm breasts. These results are in good agreement with our exposure parameters of 28 kV at 4 cm and 5 cm and 29 kV at 6 cm.

Flynn et al [5], in their simulation study, concluded that the use of a W tube rather than the traditional Mo tube should lead to significant reductions in exposure time and tube heat, while maintaining similar image quality and dose. In particular, as in our study, they found that the CNR/square root (average glandular dose) for the W/Ag combination is maximised at about 29 kV.

Conclusion

In summary, and consistent with other published data, these results demonstrate that for compressed breast thicknesses ranging from 4 cm to 6 cm and different breast glandularity, the W/Rh combination is always the best choice to deliver high performance in terms of image quality at a lower dose.

As far as the AEC of the two systems is concerned, the voltage choice of the W tube system is in good agreement with our study optimisation, whereas the voltage choice of the Mo tube system is less optimal.

References

1. Dance DR, Thilander Klang A, Sandborg M, Skinner CL, Castellano Smith IA, Carlsson GA. Influence of anode/filter material and tube potential on contrast, signal-to-noise ratio and average absorbed dose in mammography: a Monte Carlo study. Br J Radiol 2000;73:1056–67.
2. Andre MP, Spivey BA. Optimization of tungsten X-ray spectra for digital mammography: a comparison of model to experiment. Proc SPIE 1997;3032:411–18.
3. Fahrig R, Yaffe MJ. Optimization of spectral shape in digital mammography: dependence on anode material, breast thickness and lesion type. Med Phys 1994;21:1473–81.
4. Fahrig R, Yaffe MJ. A model for optimization of spectral shape in digital mammography. Med Phys 1994;21:1463–71.
5. Flynn M, Dodge C, Peck D, Swinford A. Optimal radiographic techniques for digital mammograms obtained with an amorphous selenium detector. Proc SPIE 2003;5030: 147–56.
6. Bernhardt P, Mertelmeier T, Hoheisel M. X-ray spectrum optimization of full-digital mammography: simulation and phantom study. Med Phys 2006;33:4337–49.
7. Toroi P, Zanca F, Young KC, van Ongeval C, Marchal G, Bosmans H. Experimental investigation on the choice of the tungsten/rhodium anode/filter combination for an amorphous selenium-based digital mammography system. Eur Radiol 2007;17:2368–75.
8. Williams MB, Raghunathan P, More MJ, Seibert JA, Kwan A, Lo JY, et al. Optimization of exposure parameters in full field digital mammography. Med Phys 2008;36:2414–23.
9. European Commission. European guidelines for quality assurance in breast cancer screening and diagnosis, 4th edn. (Luxembourg: Office for Official Publications of the European Communities) 2006.
10. Dance DR, Skinner CL, Young KC, Beckett JR, Kotre CJ. Additional factors for the estimation of mean glandular breast dose using the UK mammography dosimetry protocol. Phys Med Biol 2000;45:3225–40.
11. Jennings RL, Quinn PW, Gagne RM, Fewell TR. Evaluation of X-ray sources for mammography. Proc SPIE 1993;1896:259–68.
12. Lo JY, Samei E, Jesneck JL, Dobbins III JT, Baker JA, Singh S, et al. Radiographic technique optimization for an amorphous selenium FFDM system: phantom measurements and initial patient results. Proceedings of the IWDM 2004;31–6.